1 μm wavelength swept fiber laser based on dispersion-tuning technique

Jiawei Mei (梅佳伟)*, Xiaosheng Xiao (肖晓晟), and Changxi Yang (杨昌喜)

Department of Precision Instruments, Tsinghua University, Beijing 100084, China
**Corresponding author: mjw503@gmail.com*

Received May 20, 2015; accepted June 30, 2015; posted online July 30, 2015

We report a wavelength swept fiber laser at the 1 μm region based on an actively mode-locked dispersion-tuning technique. The ring-cavity laser uses a 70 cm ytterbium-doped fiber as a gain medium. Mode locking is achieved by the direct modulation of the amplitude modulator, and a ~1000 m single-mode fiber is used to provide the desired intracavity dispersion. By sine-modulating the modulation frequency, a wavelength swept laser with a range of ~30 nm can be achieved at a sweeping rate of 50 Hz. The characteristics of the laser, such as its single-wavelength tuning range, tuning sensitivity, static linewidth and sweeping rate, are also studied experimentally.

OCIS codes: 140.3510, 140.3600, 140.3615.
doi: 10.3788/COL201513.091403.

Wavelength swept lasers are versatile in sensing applications, such as fiber Bragg grating sensors[1], absorption spectroscopy measurements[2], and optical coherence tomography (OCT)[3–5]. In recent years, wavelength swept lasers in the wavelength range around 1060 nm have attracted more and more attention, and increasing interest has been found for using them in *in vivo* OCT imaging due to their special optical characteristics[6–8]. In the 1060 nm range, the water absorption is considerably lower than in the 1550 and 1300 nm bands. Besides, compared to the 800 nm band, 1060 nm laser radiation has weaker scattering and lower absorption by melanin in the retinal pigment epithelium, which permits deeper penetration into biological tissues[9,10].

Many kinds of 1 μm wavelength swept lasers have been proposed so far, and most of the schemes consist of mechanical tunable filters, such as polygonal mirror scanners[11], and piezo-tunable Fabry–Perot filters[12–14]. These filters generally have the disadvantages of high cost, bulk volume, a nonlinear mechanical response, and a limited sweep speed. Jayaraman *et al.* reported another type of 1 μm wavelength swept laser based on micro-electromechanical systems tunable vertical-cavity surface-emitting laser (VCSEL) light source technology[15]. By changing the cavity length of the VCSEL, the output wavelength can be tuned. It has the advantages of a narrow linewidth, continuous single-mode tuning, and high-speed tuning capability[15]. However, its intricate fabrication process makes it a little expensive, and its output parameters are not convenient to adjust once it has been custom-made.

Recently, a novel wavelength tuning method was proposed[16–18] based on an actively mode-locked dispersion-tuning technique. It is an actively mode-locked fiber laser in a pulsed operation that gets rid of tunable filters. The wavelength tuning method is achieved through the change of the modulation frequency in the laser cavity with large chromatic dispersion. The lasing wavelength is measured to be linearly in proportion to the modulation frequency applied to the intracavity modulator[18]. Since this technique does not require any physical tunable filters, the laser can be operated at a wide tuning range and a fast tuning speed[19]. Additionally, its output characteristics can be adjusted in a more flexible way, by tuning the intracavity parameters online[20]. By employing this technique, Wang *et al.* reported a 1 μm static, tunable, actively mode-locked fiber laser working in dissipative soliton mode for the first time in 2012[21]. But due to the small intracavity dispersion, the linewidth is so wide (~9 nm) that the coherent length is very short, which limits its application in OCT[21]. Zhang *et al.* also demonstrated a tunable fiber optical parametric oscillator operated at the 1 μm regime based on dispersion tuning in 2013[22]. The static tuning of the output wavelength can be achieved by adjusting the pump wavelength in combination with the time-dispersion-tuning technique via a mechanically tunable optical delay line[22]. However, this optical-delay-tuning method is not fit for achieving dynamic wavelength sweeping. So far, to the best of our knowledge, there is no report of 1 μm wavelength swept lasers based on a dispersion-tuning technique.

In this Letter, a wavelength swept mode-locked fiber laser based on a dispersion tuning technique at 1 μm region is reported. By tuning the modulation frequency periodically, a wavelength swept laser with a range of ~30 nm can be achieved at a sweeping rate of 50 Hz. We also study the characteristics of the single-wavelength tuning range, tuning sensitivity, static linewidth, and sweeping rate of the laser experimentally.

The experimental setup of the proposed wavelength-tunable, mode-locked fiber laser is shown in Fig. 1. It is a fiber ring laser that is actively mode locked with a lithium niobate ($LiNbO_3$) amplitude modulator designed for use in the 1 μm region. The modulator has an insertion loss of about 4 dB and a bandwidth of 2.5 GHz. The active mode locking is realized by modulating the modulator

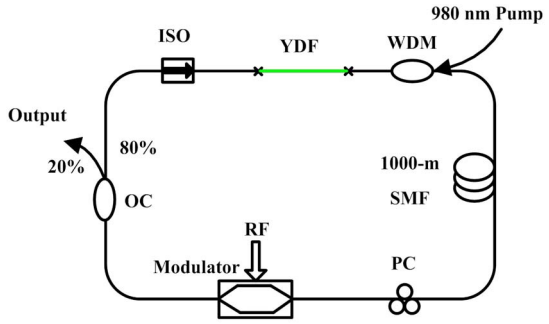

Fig. 1. Schematic diagram of the wavelength swept fiber laser based on dispersion tuning. WDM: wavelength-division multiplexer, ISO: optical isolator, OC: optical coupler.

with a radio frequency (RF) signal from a RF synthesizer (Agilent N5181A). A 70 cm ytterbium-doped fiber (YDF) with an absorption efficiency of 250 dB/m is backward pumped by a 980 nm laser diode with an output power of 200 mW, which is used as the gain medium. A polarization controller (PC) is used to optimize the polarization of the input light to the modulator. A ∼1000 m length of commercial single-mode fiber (SMF) with a normal dispersion of ~ -40 ps/nm/km at the 1 μm region and an insertion loss of less than 2 dB is introduced to provide large intracavity dispersion. An isolator ensures unidirectional light propagation in the laser cavity. Finally, 20% of the light in the laser cavity is output via a 20/80 coupler. An optical spectrum analyzer (Agilent 86142B) with a resolution of 0.06 nm and a digital oscilloscope (Agilent DSO80204B) combined with a 1 GHz photodetector (Thorlabs D400FC) are used to simultaneously monitor the output spectrum and pulse train, respectively. The total cavity length is ∼1030 m and the corresponding fundamental frequency is ∼197 kHz.

According to Ref. [16], in the dispersion-tuning regime, the derivation of the wavelength with respect to modulation frequency f_m can be written as

$$\frac{d\lambda}{df_m} = -\frac{N}{f_{m0}^2 DL}, \tag{1}$$

where f_{m0} is the central mode-locking frequency, D is the average dispersion parameter of the whole cavity, N is the harmonic mode-locking order, and L is the whole cavity length. Equation (1) shows that the harmonic mode-locking frequencies are all wavelength-dependent. Thus, when the laser is modulated at one of the harmonics, the emission wavelength can be tuned continuously by changing the modulation frequency.

If the gain bandwidth is large enough, it is known from Ref. [18] that the wavelength spacing between the Nth and the $(N+1)$th harmonic mode locking under the modulation frequency f_m can be written as

$$\Delta\lambda_N = \left|\frac{1}{f_m DL}\right|, \tag{2}$$

where $\Delta\lambda_N$ represents the wavelength spacing of two adjacent lasing channels. Therefore, if the wavelength spacing $\Delta\lambda_N$ is larger than the gain bandwidth, the laser will work in a single-wavelength operation. Assuming the gain bandwidth of our laser is ∼30 nm, according to the gain profile of the YDF and the loss spectrum of the cavity[21], which can also be confirmed by the following experiment, the critical modulation frequency f_0 to produce a single wavelength at the full gain bandwidth is calculated to be ∼1000 MHz.

According to the above theoretical analysis, we set f_m to be around 200.050 MHz, and the harmonic mode-locking order N is 1015. The wavelength spacing at this modulation frequency is calculated to be about 125 nm according to Eq. (2), much larger than the gain bandwidth. Figure 2 shows that the lasing wavelength shifts toward the longer wavelength as f_m is changed manually from 200.033 to 200.078 MHz. A total tuning range of ∼30 nm is obtained. Figures 3(a) and 3(b) depict the waveform and frequency spectrogram of the single-wavelength pulse train at a modulation frequency of 200.053 MHz, respectively. An optical signal-to-noise ratio (OSNR) greater than 50 dB is achieved.

It should be noted that the current tuning range is mainly limited by the gain bandwidth and can be further expanded by using a wider gain bandwidth medium instead of the YDF, such as a semiconductor optical amplifier (SOA)[13] or an optical parametric oscillator[22].

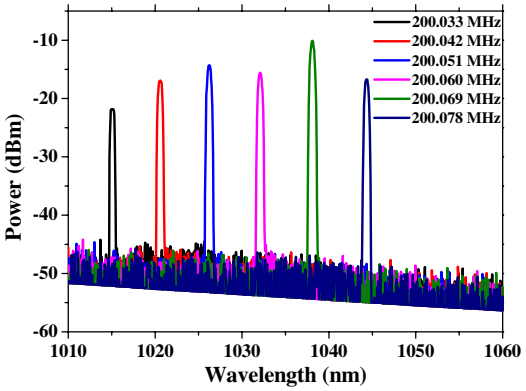

Fig. 2. Spectra of single-wavelength operation at six modulation frequencies from 200.033 to 200.078 MHz.

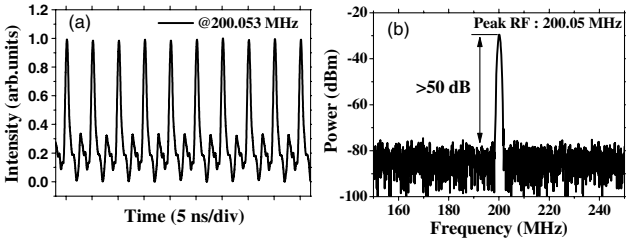

Fig. 3. (a) The pulse train of a single-wavelength operation at the modulation frequency of 200.053 MHz. (b) The corresponding frequency spectrogram of the pulse train.

For the modulation frequency of ~200 MHz ($N = 1015$), the relationship between the wavelength change and the modulation frequency change is shown in Fig. 4. The correlation coefficient is 0.99996, verifying a highly linear dependence. The slope of the fitted line is 0.650 nm/kHz. The average dispersion coefficient is derived to be −37.4 ps/nm/km using Eq. (1), which agrees well with the theoretical value.

We also measure the characteristics of the wavelength tuning at the modulation frequencies of ~50 MHz ($N = 254$) and ~500 MHz ($N = 2538$), which are also shown in Fig. 4. The corresponding slopes of the two fitted lines are 2.622 and 0.261 nm/kHz, respectively. The corresponding dispersion coefficients are calculated to be about −37.1 and −37.3 ps/nm/km. The results show that the tuning sensitivity decreases with the increase of the mode-locking order.

The linewidth of the static output spectrum is directly related to the coherence length of the wavelength swept laser, which determines the imaging depth in OCT applications[23]. So it is desirable to get a narrower static linewidth to achieve a larger imaging depth. According to Ref. [18], the linewidth of the pulse in an actively mode-locked dispersive cavity is related to the modulation frequency (mode-locking order), modulation depth, the total dispersion, and the cavity length. Among these parameters, the mode-locking order is the only one that can be easily changed in our cavity. In order to investigate the relationship between the linewidth and the mode-locking order, we measure the linewidth of seven wavelengths between 1023 and 1041 nm at modulation frequencies of ~50 MHz ($N = 254$), ~200 MHz ($N = 1015$), and ~500 MHz ($N = 2538$). The experimental results are shown in Fig. 5. It can be concluded that a narrower linewidth can be obtained by increasing the mode-locking order, which is also verified in SOA-based dispersion-tuned lasers[23].

The pulse evolution in the cavity can be explained from the view of time domain: an initial pulse without a chirp produced by the modulator is broadened by the strong

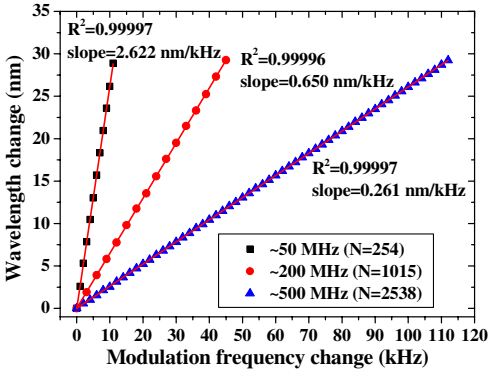

Fig. 4. The relationship between the output single wavelength and the modulation frequency change at three different mode-locking orders. The red lines are the linearly fitted lines of the experimental data.

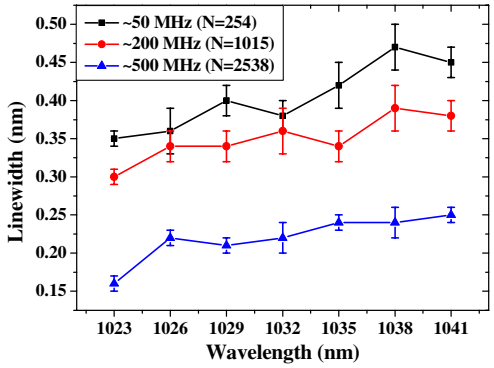

Fig. 5. The static linewidth of seven wavelengths from 1023 to 1041 nm at three different mode-locking orders.

normal dispersion of a long SMF and then goes back to the modulator again after one round trip. As the pulse is broadened with a high chirp, the time-domain intensity modulating has a significant clipping effect on the spectral pulse wings[21], similar to the dissipative soliton evolution in all-normal-dispersion (ANDi) passive mode-locked fiber lasers[24]. Therefore, the modulator just plays the combined roles of nonlinear polarization evolution and spectral filter in ANDi lasers[21,24]. Finally a Gaussian pulse profile is output with a large chirp from the laser, whose linewidth is given by[25]

$$\Delta\omega = \left(\pi \frac{f_m}{\lambda}\right)^{1/2} \left(\frac{8\pi c M}{|D|L}\right)^{1/4}, \tag{3}$$

where M is the modulation depth. Equation (3) means that the linewidth can be narrower as f_m is smaller. However, from Eq. (1), smaller f_m increases the instability of lasing wavelength and causes linewidth broadening[25], which is mostly the case in the experiments. These two effects counteract each other, causing the observed trends of the linewidth, which becomes narrower with the increase of the modulation frequency from 50 to 500 MHz.

The lasing wavelength is swept by modulating the mode-locking frequency. At the beginning, the modulation frequency f_m is set to be 200.056 MHz for the purpose of tuning the output static wavelength to be 1029.05 nm, settling at the center of the gain bandwidth. Then, a sine waveform signal is applied as a modulation signal to sweep the modulation frequency sinusoidally for a range of 46 kHz, corresponding to the wavelength range of 30 nm (1015–1045 nm). The optical spectra are measured using the optical spectrum analyzer at the peak-hold mode. Figure 6 shows the spectra obtained at different sweeping rates of 50, 200, and 1000 Hz and a dynamic tuning range of about 30 nm is achieved at 50 Hz. The ripples in the peak-hold spectra at 50 Hz are mainly because of the uneven gain spectra of the YDF. The temporal sweep waveform at a sweeping rate of 50 Hz is also measured and shown in Fig. 7.

The intensity difference between the up-scan (towards the longer wavelength) and the down-scan (towards the shorter wavelength) is believed to originate from the nonlinear effect of the long fiber[19], which needs further

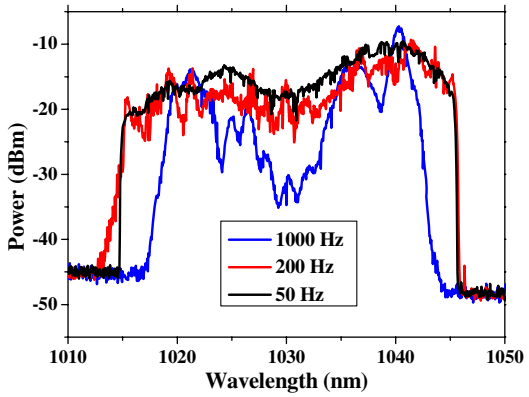

Fig. 6. The wavelength swept peak-hold spectra at three different sweeping rates of 50, 200, and 1000 Hz.

experimental investigation. It is observed that the intensity of the peak-hold spectra decreases at some wavelength range with the increase of the sweeping rate. This phenomenon occurs due to the limited photon lifetime of the long cavity, which is inversely proportional to the cavity length. For example, when the laser is swept at the rate of 1000 Hz, the laser output is suppressed at the two sides of the tuning range, and the swept range shrinks accordingly. Additionally, the ripples become more intense. Therefore, if a large wavelength swept range is acquired at high sweeping rate, the cavity should be designed to be shorter and of lower loss. So a wideband chirped fiber Bragg grating[26] is recommended to be used as the dispersive medium instead of a single-mode fiber to reduce the cavity length.

In conclusion, we demonstrate a 1 μm wavelength swept actively mode-locked fiber laser based on a dispersion-tuning technique. By employing an electro-optic modulator as an active mode-locking device and inserting a segment of SMF to increase the intracavity dispersion, the tunable single-wavelength tuning range of ~30 nm is achieved. The intensity modulator acts not only as a temporal window, but also as a spectral filter for the pulse evolution in the highly dispersive cavity. We also obtain the same sweeping range at a sweeping rate of 50 Hz by sine-modulating the modulation frequency. The single-wavelength tuning range, tuning sensitivity, and static linewidth have been characterized experimentally.

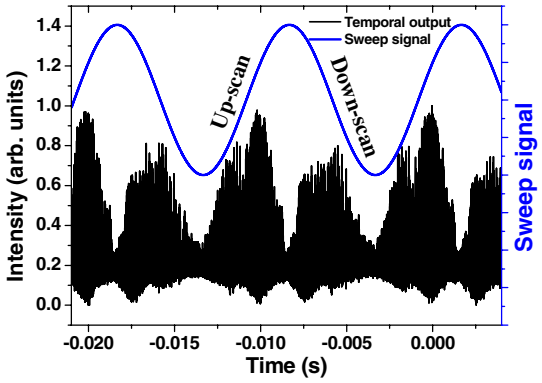

Fig. 7. The temporal sweep output at the sweeping rate of 50 Hz. The blue line is the sinusoidal sweep signal.

This work was supported by the Importation and Development of High-Caliber Talents Project of Beijing Municipal Institutions (No. YETP0089) and the National Natural Science Foundation of China (Nos. 61377039 and 61177046).

References

1. S. H. Yun, D. Richardson, and B. Y. Kim, Opt. Lett. **23**, 843 (1998).
2. H. Y. Ryu, W. K. Lee, H. S. Moon, and H. S. Suh, Opt. Commun. **275**, 379 (2007).
3. R. Huber, M. Wojtkowski, and J. G. Fujimoto, Opt. Express **14**, 3225 (2006).
4. T. Wu and Y. Liu, Chin. Opt. Lett. **11**, 021702 (2013).
5. G. Liu and R. Wang, Chin. Opt. Lett. **11**, 031701 (2013).
6. B. Potsaid, B. Baumann, D. Huang, S. Barry, A. E. Cable, J. S. Schuman, J. S. Duker, and J. G. Fujimoto, Opt. Express **18**, 20029 (2010).
7. S. Marschall, T. Torzicky, T. Klein, W. Wieser, M. Pircher, E. Gotzinger, S. Zotter, M. Bonesi, B. Biedermann, C. Pedersen, R. Huber, C. Hitzenberger, and P. E. Andersen, Proc. SPIE **8427**, 84271D (2012).
8. T. Torzicky, S. Marschall, M. Pircher, B. Baumann, M. Bonesi, S. Zotter, E. Götzinger, W. Trasischker, T. Klein, W. Wieser, B. Biedermann, R. Huber, P. Andersen, and C. K. Hitzenberger, J. Biomed. Opt. **18**, 026008 (2013).
9. B. Povazay, K. Bizheva, B. Hermann, A. Unterhuber, H. Sattmann, A. F. Fercher, W. Drexler, C. Schubert, P. K. Ahnelt, M. Mei, R. Holzwarth, W. J. Wadsworth, J. C. Knight, and P. S. J. Russel, Opt. Express **11**, 1980 (2003).
10. A. Unterhuber, B. Považay, B. Hermann, H. Sattmann, A. Chavez-Pirson, and W. Drexler, Opt. Express **13**, 3252 (2005).
11. S. W. Lee, H. W. Song, M. Y. Jung, and S. H. Kim, Opt. Express **19**, 21227 (2011).
12. J. Zhang, Q. Wang, B. Rao, Z. Chen, and K. Hsu, Appl. Phys. Lett. **89**, 073901 (2006).
13. S. Marschall, T. Klein, W. Wieser, B. R. Biedermann, K. Hsu, K. P. Hansen, B. Sumpf, K.-H. Hasler, G. Erbert, O. B. Jensen, C. Pedersen, R. Huber, and P. E. Andersen, Opt. Express **18**, 15820 (2010).
14. T. Klein, W. Wieser, C. M. Eigenwillig, B. R. Biedermann, and R. Huber, Opt. Express. **19**, 3044 (2011).
15. V. Jayaraman, G. Cole, M. Robertson, C. Burgner, D. John, A. Uddin, and A. Cable, Electron. Lett. **48**, 1331 (2012).
16. S. Li and K. T. Chan, IEEE Photon. Technol. Lett. **10**, 799 (1998).
17. K. L. Lee, K. Chan, and C. Shu, IEEE Photon. Technol. Lett. **13**, 106 (2001).
18. S. Yamashita and M. Asano, Opt. Express **14**, 9399 (2006).
19. Y. Nakazaki and S. Yamashita, Opt. Express **17**, 8310 (2009).
20. B. Burgoyne and A. Villeneuve, Proc. SPIE **7580**, 758002 (2010).
21. R. Wang, Y. Dai, L. Yan, J. Wu, K. Xu, Y. Li, and J. Lin, Opt. Express **20**, 6406 (2012).
22. L. Zhang, S. Yang, P. Li, X. Wang, D. Gou, W. Chen, W. Luo, H. Chen, M. Chen, and S. Xie, Opt. Express **21**, 25167 (2013).
23. R. F. Stancu, D. A. Jackson, and A. G. Podoleanu, IEEE Photon. Technol. Lett. **26**, 1629 (2014).
24. P. Grelu and N. Akhmediev, Nat. Photon. **6**, 84 (2012).
25. S. Yamashita, Y. Nakazaki, R. Konishi, and O. Kusakari, J. Sensors **2009**, 1 (2009).
26. Y. Takubo and S. Yamashita, Opt. Express **21**, 5130 (2013).